3D MODELING FOR HISTORICAL STRUCTURE USING TERRESTRIAL LASER RANGING DATA

Hiroshi YOKOYAMA , Hirofumi CHIKATSU
Tokyo Denki Univ., Dept. of Civil Eng.,
Hatoyama, Saitama, 350-0394 JAPAN
E-mail: {yokoyama, chikatsu}@g.dendai.ac.jp

Commission V, WG V/4

KEY WORDS: Cultural Heritage, Modeling, Visualization, Laser scanning, Representation, Three-dimensional, Digital

ABSTRACT:

Recently, a laser scanner has been receiving more attention as a useful tool for real-time 3D data acquisition, and various applications such as city modeling, DTM generation and 3D modeling of cultural heritage were proposed.

However, 3D Representation of historical structures from point cloud 3D data collected by laser scanner is still issues. In order to reduce the time, labor and skill for archival recording of the cultural heritage, the authors discuss measuring system using 3D scanner and 3D modeling.

This paper describes on 3D representation of historical structure using laser scanner and break-line by flatness.

1. INTRODUCTION

With respect to recording work, it is essential to reduce the amount of time, labor, and skill employed while making archival records of a historical structure. In order to do so a laser scanner is used to measure the sites, and on the basis of the results, an image of the model is constructed.

The Triangulated Irregular Network (TIN) model is generally generated for 3D modeling using all the measured points[1)], however, the large amount of point cloud data obtained by the laser scanner pose a problem.

Although the Marching Cube Algorithm is generated for reduction of the data values or the polygon number, the precision setting of the model changes.

This issue becomes a particularly serious problem in accurate 3D modeling. In this paper, the 3D modeling of a historical structure, using a laser scanner and break-lines will be introduced.

2. 3D REPRESENTATION

Figure 1 presents a flowchart of certain processes for the 3D representation of the historical structure. Recently, the laser scanner has attracted considerable attention as a measurement tool that can perform extensive 3D measurements in a short time. A Total Station is often used for this purpose, but it requires a greater amount of measurement time, labor, and skill as compared with the laser scanner. Hence, the authors measured the historical structure and carried out 3D modeling using laser scanners to save time and labor. Additional technical outlines are presented later.

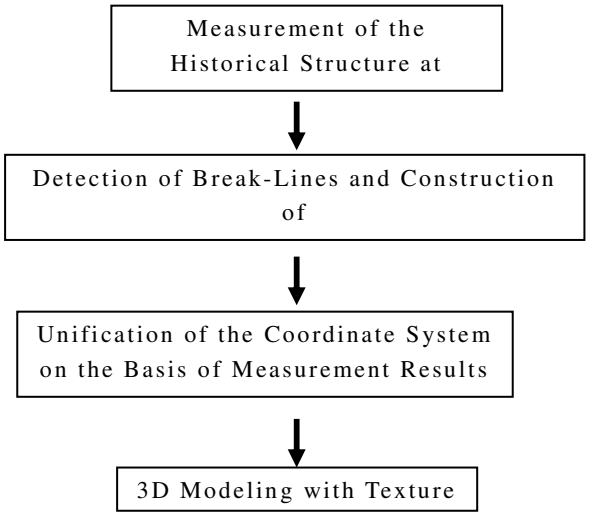

Fig.1 Flowchart for 3D Representation

3. 3D MODELINGN USING BREAK-LINES

3.1 Outline of Modeling Process

The historical structure consists of several flat parts. Therefore, its 3D modeling is enabled by the unification of all flat parts in the 3D

model. Next, the break-lines provide the object edges and, ridgelines, and these can used to accurately determine the points to be modeled of the TIN along with the flatness classification results. The technical outlines are presented later.

3.2 Classification of The Flat and Non-Flat Areas

In order to develop a robust filtering method for topographic surveying, 3D point cloud data for a topographic scene was acquired using a terrestrial laser scanner. A small mask with 30*30 cm area is used instead of the 3D information samples. After a 3*3 point mask is generated around an interest point, the mask size expands to 30*30 cm by computing the plane coordinates for the neighbor points.The mask is then transformed so that in the first step, a normal vector for the mask becomes parallel to the Z-axis (Figure 2). In the next step, the Standard Deviation (S.D.) is computed for the interest point. The threshold value should be considered while classifying the interest points into flat (ground surface, structure walls, etc.,) and non-flat areas (trees, bushes, sky, etc.). The threshold value is determined on the basis of the measured data.

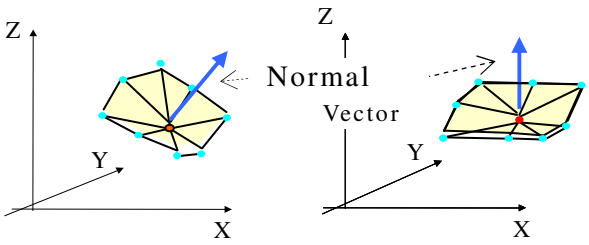

Fig.2 Coordinate Transformation

However, the ends of the big slopes are classified as non-flat points. Figure 3 shows example of flat and non-flat points in the big slopes. In order to resolve the second issue, the following procedures were created, and the authors termed this process as "S.D. Saving".

The S.D. Saving Process:

+ If an interest point is detected as topographic data, the Z values of all the points in the mask are compared with the S.D. values.

+ If the Z values of each point are smaller than the S.D. values of the interest point, then these points are recorded as topographic data.

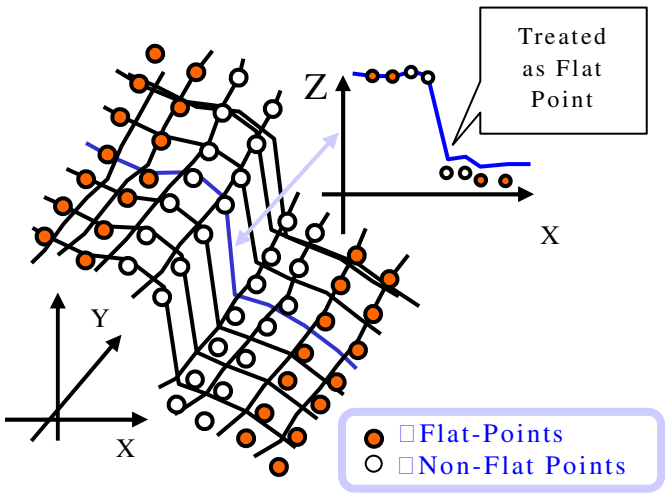

Fig. 3 Examples of Flat and Non-Flat Points

3.3 Derivation of the Break-Lines

The break-lines (e.g., object edges, ridge-lines) provide important morphological information. Although these are indispensable features for DTM generation, city and object modeling, problems with automatic detection of the break-lines still persist. A technique for automatic detection of the break-lines using the flatness values was developed[5]. The algorithm is closely related to edge-preserving smoothing;, however, only the flat area is smoothened, and points with a larger S.D. within the non-flat area are emphasized. A small mask was used for smoothening. A mask size of 30*30 cm was sufficient, and an interest point was smoothened using the following equation:

$$g_j = \frac{\sum p_i \cdot \Delta g_{i,j}}{\sum p_i} \qquad (1)$$

where,

g_j: S.D. for an interest point,

$\Delta g_{i,j}$ ::Difference in S.D. between an interest point and its neighboring points;,

defined as $\Delta g_{i,j} = g_i - g_j$,

p_i: Weight of the i point; where the weight is defined as the square of the values between the interest point and each neighboring point.

In order to detect the break-lines, smoothening of only the flat areas is repeated. Repeating this three times was sufficient, and the points with a larger standard deviation within the non-flat areas were emphasized.

As a result, the break-lines were derived, and these are shown in Figure 4, and figure 5 presents break-line detection for historical structure.

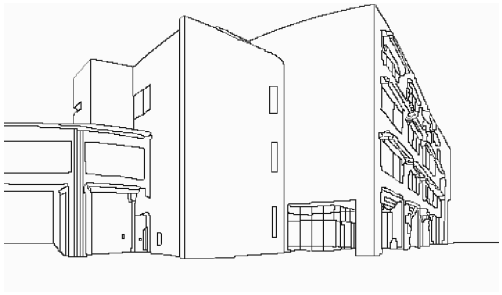

(a) Detected break-lines by manually

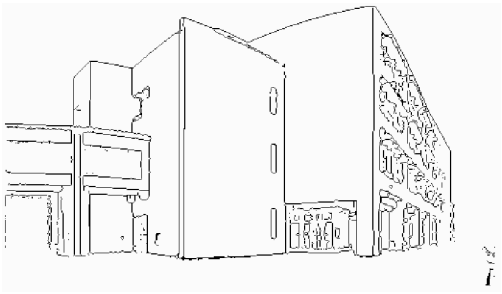

(b) Break-lines detection by the developed method

Fig.4 Detection of The Break-line for efficiency certification

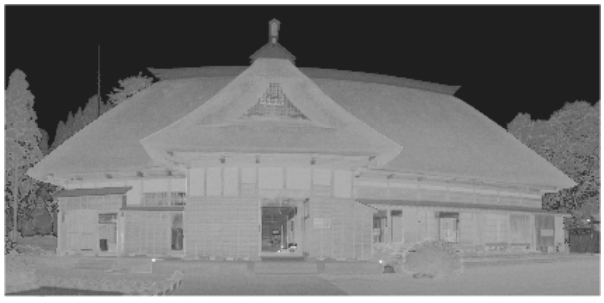

(a)Measurement Result (Intensity Data)

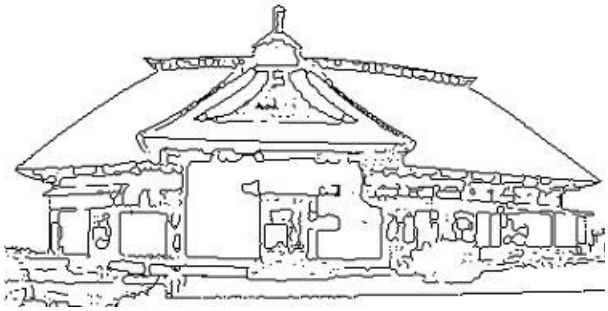

(b) Detected Break-lines by the developed method

Fig.5 Detection of The Break-Lines for Historical Structure

3.4 Recognition of Standard Deviation for Classification of the Flat Area

The threshold of flatness was classified on the basis of the measurement results. Figure 6 shows the measurement targets for reference, and figure 7 presents the S.D. values for some mask sizes.

In this paper, the threshold was set at S.D. = 0.020 m (inclusive of rough unpaved roads), which considered the state of the roof surfaces (comprising of straw).

The gray part in figure 8 indicates the flat area that is a result of the classification using the results indicated in figure 5(a). The white part indicated the flat area by "S.D. Saving".

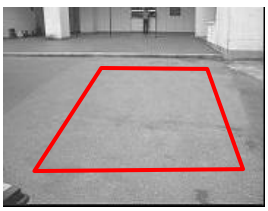

(a) Paved Road

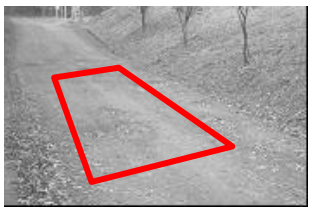

(b) Rough Unpaved Road

(c) Roadside Barrier (d) Shrubbery

: Reference Area

Fig.6 The Measurement Targets for Reference.

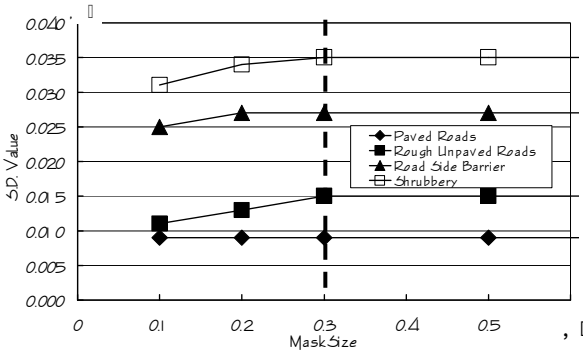

Fig.7 The S.D. Values for Some Mask Sizes

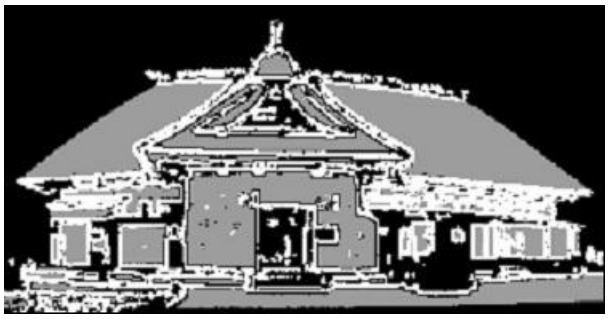

Fig.8 Classification Result of the Flat Part

The omitted parts were confirmed to be uneven parts (e.g., the upper part of the roof), therefore, the second flatness and additional classification of the uneven parts were performed. In this paper, the second threshold was set at S.D. = 0.030 m (inclusive of the road side barrier), and figure 9 shows the result of the classification using the second threshold.

With this work, classification of what constitutes a cultural heritage is complete, and figure 10 present the all result of classification as flat area.

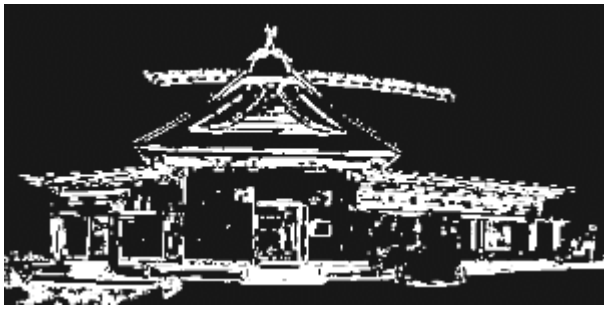

Fig.9 The Result of Classification for the Second Threshold

Fig.10 The Result of Classification as Flat Area (Color: Intensity DATA)

3.5 Extraction of the Curved Point

After the classification of the flat and non-flat areas, the shape of each area is obtained by tracing the circumference.

When all points on the circumference are used, a large number of data values (number of points for modeling) are obtained. Therefore, the points that would be used to design the model must satisfy the following conditions. They were extracted from the point crowd data to constitute the area.

The conditions for point extraction:

a. Curved point of the circumference

b. Point on the Circumference (randomly extracted)

c. Point inside of the area (randomly extracted)

b. and c. are extracted by smooth shape correspondence, and the method used for the "curved point of the circumference" is presented later.

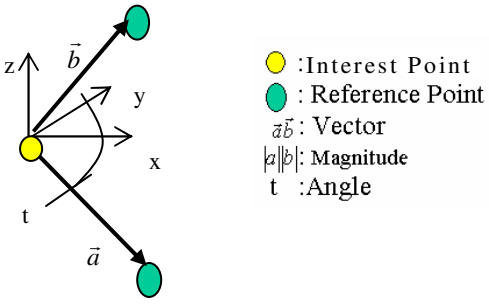

Fig.11 Conception of Inner Product

$$\vec{a}\vec{b} = |a||b|\cos t \qquad (2)$$

where,

$\vec{a}, \vec{b}$ =Vector, $|a|, |b|$ =Magnitude(Distance

of reference point and Interest point),

t = Angle

$$\vec{ab} = (Xi - Xa)(Xb - Xi) + (Yi - Ya)(Yb - Yi) + (Zi - Za)(Zb - Zi)$$

(Xi, Yi, Zi) =Position data of interest point,

(Xa, Ya, Za) =Position data of reference point,

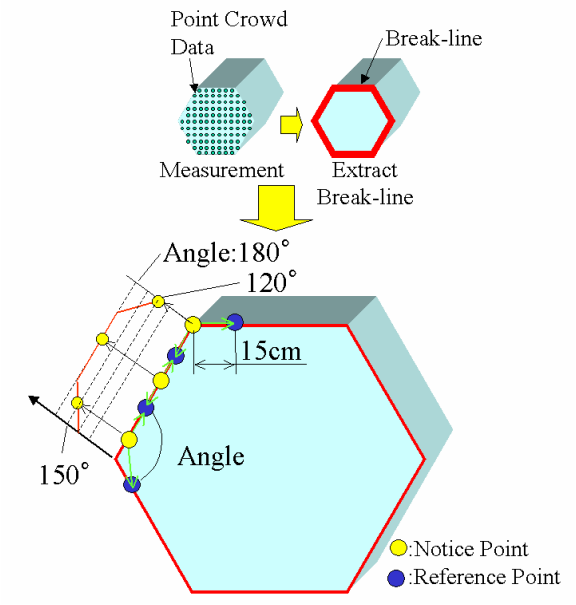

(a) Angle Calculated for One Side

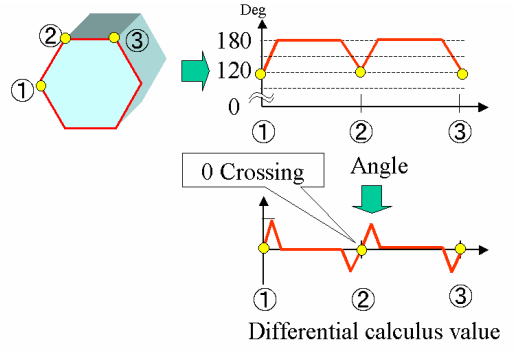

(b) Angle Calculated for Some Side

Fig.12 The Calculated Result of The Angle at The Circumference

" Curved point of the circumference " is extracted using the principle of the inner product used in a vector. Figure 11 and the equation 2 present the inner product.

First, the angle between the vectors in 3D space, which is used in the inner product, is calculated using the 3D data of the interest point and the two reference points. Distance of the interest point and the reference point is set with 15cm, and this distance is classified on the basis of the mask size. The differential calculus value is calculated just before the angle value.

Figure 12 presents the results of the calculation of the angle at the circumference. When the crossing of the difference share value becomes 0, the curved points can be found at the 0 crossing point. Therefore, in this process, the curved point of the circumference is automatically extracted. Figure 13 shows the result when the method was applied by real data.

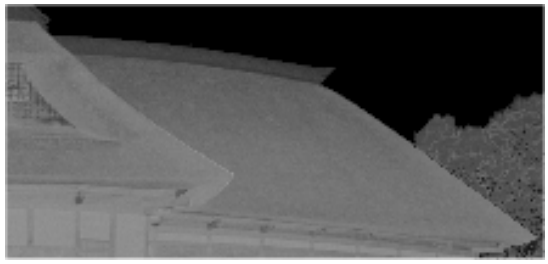

(a) Target Area (Intensity Image)

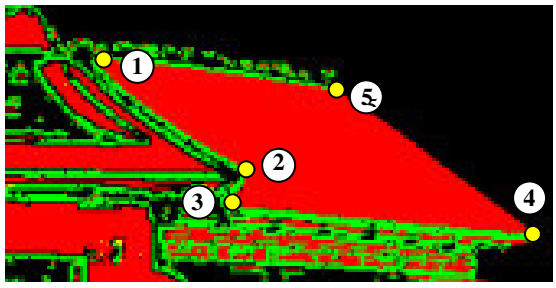

: Curved Point

(b) Classified Result as Flat Part

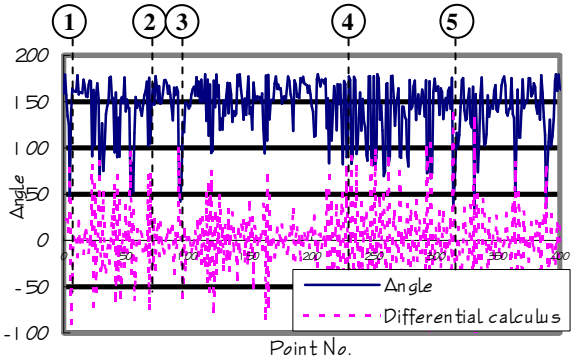

(c) Calculated Result about Angle in Flat Part

Fig.13 Calculation Result of The Angle in Real Data

From this figure, frequent angle change by error of measurement results is confirmed, and a lot of points are extracted by 0 crossing.

Thus the mean of angle data with attention point and point of surroundings (each two points of front and back) was calculated, and differential value was demanded. Figure 14 present calculation result of the angle using the result of calculated mean, and 0 crossings at curve point are confirmed. Unnecessary points to make 3D model are reduced by this work.

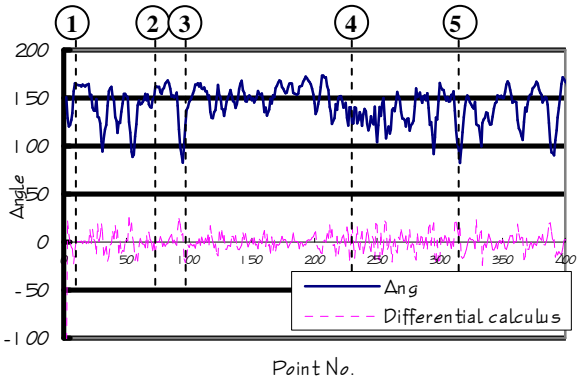

Fig.14 Calculation Result of The Angle in consideration of the mean

3.6 The Modeling Method

The curved points and the circumference points are at the circumference of the flat area, however, they may not be at the edge of the object being measured. Thus, the points on the circumference are confirmed by the existence of the break -line at the circumference. Further, when there is a break -line, the point is moved on the break-line. Figure 15 present the movement of the circumstance points.

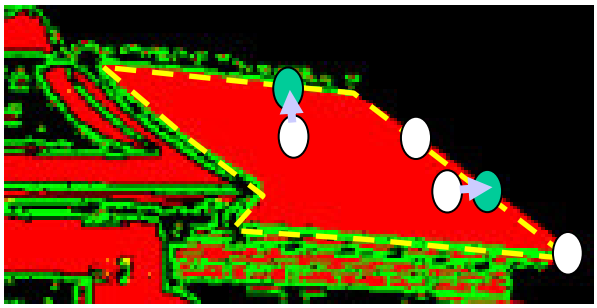

Fig.15 Movement of Circumstance Points

After these processes, the TIN model was constructed made using the curved point of the circumference, the circumference (randomly extracted), and the points inside the area (randomly extracted).

4. UNIFICATION OF COORDINATE SYSTEM BY MEASUREMENT RESULTS

In general, many lack of data which are caused by blind parts are estimated from a measurement result. Then, measurements at multiple places become needed. Due to the lack of data, the authors have been concentrating on developing visual traverse system in topographic survey[6]. In the visual traverse system, coordinate systems for multiple measurements were unified automatically.

Authors used the system to unify coordinate systems in this paper.

5. 3D MMODELING USING MULTIPLE MEASUREMENT RESULTS

3D Modeling for the "Megro residence" was investigated in this paper as one of applications using break-line. The Megro residence was constructed in 1797 (about 200 years ago). The house was the residence of “warimotoshoya” (headman of the villages in this area), and the main characteristic is the “chidorihafu” style in front roof window which was used as a chimney and added magnificence to the house. The house was designated as national important cultural assets in 1971. Figure 16 presents 3D model

obtained by multiple measurement results. Followings are the major contents for the measurement area.

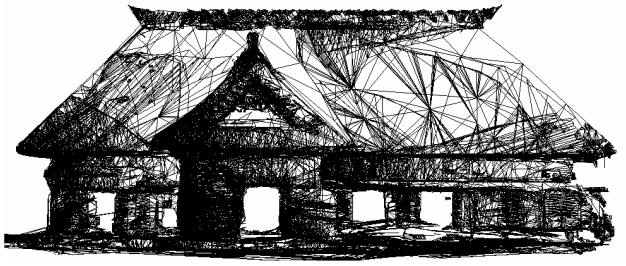

(a) Wire-flame Model

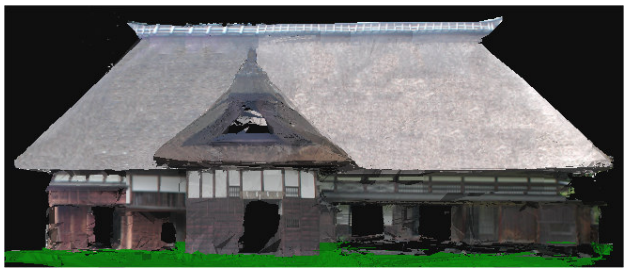

(b) Textured Model

Fig.16 3D model Obtained by Multiple Measurement Results

+ Target: Meguro Residence
+ Measurement Area: 40m*40m
+ Traverse Point: 8 points
+ Length for Leg of Traverse:200m
+ Accuracy of Traverse: 1/8,300

6. CONCLUSION

The most remarkable points as results of this approach are its ability to 3D modeling image often give important information for historical investigation.

As for further additional results of this investigation, ability improvement of the curve point detection using break line and utility of break-line to another targets can be archived. Therefore, we'll continue examination about automatic unification method of coordinate systems and effective modeling method.

REFERENCES

1.HUAN Y-P, 1989, Triangular irregular network generation and topographical modeling, Computer in industry, pp.203-213

2.W.E.Laurensen, H.E.Cline,1987, Marching Cubes: A High Resolution 3D Surface Construction Algorithm, Proc. ACM SIGGRAPH '87,ACM Press,163-169

3.H.YOKOYAMA, H.CHIKATSU, 2003, 3D Representation of Historical Structure for Digital Archives by Laser Scanner, IAPRS, Vol.XXXIV, Part 5/W12,Ancona, Italy, pp. 347-350.

4.Brugelmann, R., 2000. Automatic breakline Detection from sairborne Laser Range Data. IAPRS, Vol.XXXIII, Part B3, Amsterdam, The Netherlands, pp. 109-116.

5.H.CHIKATSU, H.YOKOYAMA, 2003, Robust Filtering for Topographic Surveying by Terrestrial Laser Scanner, Optical 3D Measurement techniques VI, Vol. I, pp.338-345

6.R.Tanaka, H.Yokoyama, H.Chikatsu, 2002, Study on Visual Traverse by Laser Scanning Sensor, International Archives of Photogrammetry and Remote Sensing, Vol.34, Part 5, pp.95-98.

7.David C. Kay, John. R. Levine, 1995, Graphics File Formats Second edition, McGraw-Hill, Inc.